Original Article

DOI: 10.5582/bst.2025.01178

Survival benefit of adjuvant chemotherapy and individualized prognosis in resected cHCC-CCA

Bo Sun[1,2,§], Yimeng Wang[1,3,§], Ruyu Han[1,3], Yuren Xia[1,4], Meng Zhao[1,5], Liyu Sun[1,3], Xiaochen Ma[1,3], Tianqiang Song[1,3], Xiangdong Tian[1,6,*], Wenchen Gong[1,7,*], Lu Chen[1,3,*]

[1] Tianjin Medical University Cancer Institute and Hospital, National Clinical Research Center for Cancer, National Key Laboratory of Druggability Evaluation and Systematic Translational Medicine, Tianjin Key Laboratory of Digestive Cancer, Tianjin's Clinical Research Center for Cancer, Tianjin, China;
[2] The Second Department of Breast Cancer, Tianjin Medical University Cancer Institute and Hospital, Tianjin, China;
[3] Department of Hepatobiliary Cancer, Liver cancer research center, Tianjin Medical University Cancer Institute and Hospital, Tianjin, China;
[4] Department of Pediatric Oncology, Tianjin Medical University Cancer Institute and Hospital, Tianjin, China;
[5] Department of Clinical laboratory, Tianjin Medical University Cancer Institute and Hospital, Tianjin, China;
[6] Department of Endoscopy, Tianjin Medical University Cancer Institute and Hospital, Tianjin, China;
[7] Department of Pathology, Tianjin Medical University Cancer Institute and Hospital, Tianjin, China.

SUMMARY: Combined hepatocellular-cholangiocarcinoma (cHCC-CCA) is a rare malignancy with poor prognosis and unclear benefit from adjuvant chemotherapy. To identify the appropriate candidates for postoperative adjuvant chemotherapy in cHCC-CCA, we developed a prognostic model to predict patient outcomes and stratify populations accordingly. This retrospective study included 75 cHCC-CCA patients treated at Tianjin Medical University Cancer Institute and Hospital from 2009 to 2019. Prognostic factors were identified via univariate and multivariate Cox regression. Model performance was assessed using ROC curves, calibration plots, and decision curve analysis. Propensity score matching (PSM) was applied to reduce bias. Adjuvant chemotherapy significantly improved overall survival (OS) in Kaplan–Meier (p = 0.029) and PSM analyses (p = 0.0011). Five independent prognostic factors were identified: macrovascular invasion, lymph node metastasis, the largest tumor size >5 cm, the high expression of CD8, and the high expression of FOXP3. The nomogram showed good predictive performance. Among high-risk patients stratified by the nomogram, those receiving adjuvant chemotherapy had longer OS (p = 0.013), while no significant benefit was observed in the low-risk group (p = 0.084). Adjuvant chemotherapy improves postoperative survival in cHCC-CCA. The nomogram provides individualized risk stratification and may inform treatment decisions.

Keywords: cHCC-CCA, adjuvant chemotherapy, prognostic nomogram, overall survival, propensity score matching

1. Introduction

cHCC-CCA is a rare primary liver malignancy characterized by the dual histopathological features of hepatocellular carcinoma (HCC) and cholangiocarcinoma (CCA) (*1-4*). Despite its relatively low incidence, cHCC-CCA demonstrates highly aggressive biological behavior due to its pronounced molecular and histological heterogeneity (*5-10*). As a result, CHC patients have a higher postoperative recurrence rate and significantly worse long-term survival compared to individuals with either HCC or CCA alone. Surgical resection currently stands as the sole potentially curative treatment for cHCC-CCA (*11,12*). However, the postoperative recurrence rate surpasses 50%, and the absence of standardized adjuvant treatment strategies poses a significant challenge to enhancing long-term survival outcomes for these patients (*1,13-15*).

In recent years, adjuvant chemotherapy has been extensively demonstrated to markedly enhance the prognosis of different solid tumors post-surgery (*16-18*). However, the clinical use of adjuvant chemotherapy in cHCC-CCA is contentious due to the insufficient high-quality supporting evidence. This issue is partly due to the rarity of cHCC-CCA and limited disease-specific understanding (*19*). In addition, reliable prognostic models based on large-scale real-world data are lacking, making it difficult to accurately identify appropriate candidates for adjuvant therapy and predict therapeutic efficacy (*12*).

With the progress in precision medicine, creating personalized postoperative management plans for patients with cHCC-CCA is now a pressing clinical

concern (*20-22*). Nomograms, which are practical predictive tools based on multivariate analysis, can combine clinicopathological features and molecular biomarkers to offer personalized quantitative survival predictions (*23*). While nomograms have been widely used to assess prognosis in different cancers, there is currently no validated nomogram model for predicting postoperative survival in patients with cHCC-CCA. Consequently, the potential clinical utility of nomograms in guiding adjuvant treatment decisions for cHCC-CCA remains unexplored (*24*).

In this study, we systematically reviewed the clinical and follow-up data of 75 patients with cHCC-CCA who underwent curative resection at Tianjin Medical University Cancer Institute and Hospital between 2009 and 2019. We successfully developed a prognostic nomogram model with strong predictive performance by combining conventional clinicopathological characteristics with tumor immune microenvironment indicators based on rigorous univariate and multivariate Cox regression analyses. This model accurately predicted 2-year and 3-year survival probabilities and demonstrated practical clinical utility through decision curve analysis (DCA). Additionally, using propensity score matching (PSM), we confirmed the survival benefit of adjuvant chemotherapy across different risk strata.

The study findings offer strong evidence to support individualized postoperative management and adjuvant treatment decision-making for patients with cHCC-CCA. This support may advance the clinical application of precise therapeutic strategies, leading to enhanced long-term survival outcomes in this complex patient group.

2. Materials and Methods

2.1. Patient selection

This retrospective study included 75 patients diagnosed with combined hepatocellular-cholangiocarcinoma (cHCC-CCA) who underwent curative resection at Tianjin Medical University Cancer Institute and Hospital between January 2009 and December 2019. The study was approved by the institutional ethics committee (Approval ID: bc20240058), and all participants provided written informed consent. The study was conducted in accordance with the Declaration of Helsinki. All patients had pathologically confirmed cHCC-CCA without evidence of distant metastasis or macrovascular invasion, and complete follow-up data were available.

Inclusion criteria were as follows (A-E):
A. Age ≥ 18 years.
B. Pathological confirmation of cHCC-CCA.
C. Underwent curative (R0) resection.
D. Availability of complete clinical and follow-up data.
E. No macrovascular invasion or distant metastasis at diagnosis.

Exclusion criteria were as follows (A-D):
A. Follow-up duration less than 1 month.
B. History of other malignancies.
C. Non-R0 resection.
D. Incomplete clinical data.

2.2. Data collection

Clinical data were collected retrospectively, including (A-F):
A. Demographic information: sex, age, HBV infection, and Liver cirrhosis.
B. The liver function parameters included albumin (ALB), total bilirubin (TBIL), and prothrombin time (PT).
C. Tumor characteristics included the largest tumor size, microvascular invasion, presence of satellite nodules and CD8, CD20, FOXP3, PD-L1 expression level.
D. Serum tumor markers included alpha-fetoprotein (AFP).
E. Treatment information: whether adjuvant chemotherapy was administered.
F. Follow-up data: overall survival (OS) and survival status.

2.3. Survival analysis

Survival curves were produced utilizing the Kaplan–Meier method, and group differences were evaluated through the log-rank test. OS was defined as the time from the surgery date to the death date or last follow-up. Survival differences between the adjuvant chemotherapy and non-chemotherapy groups were examined in the total cohort (n = 75), within risk-level-stratified subgroups, and in the PSM-matched cohort. Statistical significance was determined as a two-sided P-value of < 0.05.

2.4. Quantification of immune cell infiltration in tumor tissues of patients with cHCC-CCA

Immune cell infiltration in tumor tissues was quantified using formalin-fixed paraffin-embedded (FFPE) samples from patients with cHCC-CCA. Ten high-power fields (HPF, ×200 magnification) were randomly chosen for each patient to guarantee unbiased sampling. Immunohistochemical (IHC) staining with validated markers specific to immune cell populations was used to identify immune cells. Positively stained cells with distinct membrane and cytoplasmic patterns were manually counted in each field. The average count of immune cells per HPF was calculated for each patient, and an overall mean immune cell density was calculated to establish a stratification threshold. Patients were then grouped into categories (*e.g.*, high *vs*. low immune cell infiltration) based on comparisons with this threshold. This standardized approach ensures reproducibility and facilitates the evaluation of immune microenvironment

heterogeneity in cHCC-CCA.

2.5. Identification of prognostic factors and nomogram construction

Univariate Cox proportional hazards regression analysis was employed to identify potential prognostic factors for OS, with a screening threshold set at $p < 0.157$ to prevent the exclusion of crucial variables (*25*). Variables with $p < 0.157$ were subsequently included in multivariate Cox regression analysis to determine independent prognostic factors. Following these findings, five variables (macrovascular invasion, lymph node metastasis, largest tumor size > 5 cm, CD8 expression, and FOXP3 expression) were integrated into the final nomogram for predicting the probabilities of 2- and 3-year survival.

The postoperative risk score for cHCC-CCA is determined by the following formula: 44.88 × (the largest tumor size) + 59.65 × (the high expression of FOXP3 status) + 100 × (the low expression of CD8 status) + 65.2 × (major vascular invasion status) + 80.53 × (lymph node metastasis status). In this scoring system, variables are assigned numerical values according to specific criteria (A-F).

A: The largest tumor size: 1 if > 5 cm, 0 if ≤ 5 cm;
B: FOXP3 status: 1 if high expression, 0 if low expression;
C: CD8 status: 1 if low expression, 0 if high expression;
D: Major vascular invasion: 1 if present, 0 if absent;
E: Lymph node metastasis: 1 if present, 0 if absent.
F: Patients were categorized into high-risk (total score > 130) or low-risk (total score ≤ 130) groups according to their cumulative scores.

2.6. IHC staining

Consecutive sections of FFPE tissues were prepared and processed using a Ventana BenchMark XT apparatus (Ventana Medical Systems). The sections underwent dewaxing, followed by antigen retrieval at 95°C for 30 min in EDTA repair solution. Subsequently, the sections were exposed to primary antibodies against CD8 (SP57, Ventana Medical Systems, Tucson, AZ, USA), CD20 (L26, Ventana, Tucson, AZ, USA), FOXP3 (236A/E7, ab20034, Abcam, Cambridge, UK), and programmed death ligand 1 (PD-L1) (SP263, Ventana, Tucson, AZ, USA) at 37°C for 32 min. Following this, the sections were treated with an HRP-conjugated secondary antibody (multimer HRP, Ventana) for 10 min at room temperature. Positive signals were detected using diaminobenzidine and then counterstained with hematoxylin.

2.7. Evaluation of model performance

The nomogram's calibration performance was evaluated by generating calibration curves from 100 bootstrap resamples, showing strong agreement between the predicted and observed survival outcomes.

To assess the clinical utility of the model, DCA was conducted to evaluate the net clinical benefit over a range of threshold probabilities. The nomogram consistently showed superior clinical decision-making advantages in comparison to the traditional staging system for both 2-year and 3-year survival predictions.

2.8. PSM

To reduce potential confounding variables affecting the assessment of adjuvant chemotherapy, PSM was utilized to equalize the baseline characteristics between the chemotherapy and non-chemotherapy cohorts. The propensity scores were calculated using clinical and pathological variables, including sex, age, HBV infection status, presence of cirrhosis, the largest tumor size, satellite nodules, microvascular and macrovascular invasion, lymph node metastasis, and immune markers.

A 1:2 nearest-neighbor matching algorithm was utilized, yielding a matched cohort of 19 patients in the chemotherapy group and 38 patients in the non-chemotherapy group. The baseline characteristics post-matching were adequately balanced ($p > 0.05$).

Subsequent survival analysis was conducted on the matched cohort to further confirm the survival advantage of adjuvant chemotherapy after accounting for confounding variables.

2.9. Software

All statistical analyses were conducted using R software (version 4.4.3) and SPSS software (version 29.0). Nomogram construction and validation utilized the R packages "rms", "survival", and "timeROC". Calibration curves were generated through bootstrap resampling. The DCA was conducted using the "ggDCA" package. All statistical tests were two-sided, with significance set at $p < 0.05$.

3. Results

3.1. Patient enrollment and study flow

This retrospective cohort study was conducted at Tianjin Medical University Cancer Institute and Hospital, involving patients diagnosed with cHCC-CCA who underwent curative resection from January 2009 to December 2019. Following rigorous inclusion and exclusion criteria, the final analysis comprised 75 patients.

Among these patients, 19 (25.3%) received adjuvant chemotherapy, while 56 (74.7%) did not. Comprehensive clinicopathological characteristics and follow-up data were gathered, and long-term follow-up was conducted

to assess the impact of adjuvant chemotherapy on OS. Histopathologic and immunophenotypic analyses confirmed the biphenotypic differentiation of the tumor, with both hepatocellular and cholangiocellular components identified (Figures 1A-G). The overall workflow of patient screening, inclusion, and cohort analysis is summarized in a schematic diagram (Figure 1H).

3.2. Efficacy of adjuvant chemotherapy

Kaplan–Meier survival analysis revealed that patients who received adjuvant chemotherapy had a significantly better OS compared to those who did not receive adjuvant chemotherapy (p = 0.029; Figure 2A). PSM was used to mitigate potential confounding factors influencing the evaluation of adjuvant chemotherapy. Following matching, 57 patients were enrolled, with 19 and 38 patients in the chemotherapy and non-chemotherapy groups, respectively. The baseline characteristics after matching were well balanced (Table 1).

The proportion of male patients was 73.7% in the chemotherapy group and 84.2% in the non-chemotherapy group (p = 0.553). The median age was 54 years (IQR: 49–65) and 55.5 years (IQR: 52–63) in the two groups, respectively (p = 0.617). HBV infection rates (68.4% *vs*. 68.4%, p = 0.838) and cirrhosis rates (31.6% *vs*. 36.8%, p = 0.695) were similar between the two groups.

No significant differences were noted in laboratory parameters, such as ALB, TBIL, and PT. The percentage of patients with AFP levels > 40 ng/mL was 31.6% in the chemotherapy group and 57.9% in the non-chemotherapy group (p = 0.061).

There were no significant differences between the two groups regarding satellite nodules (15.8% *vs*. 21.1%, p = 0.906), microvascular invasion (5.3% *vs*.

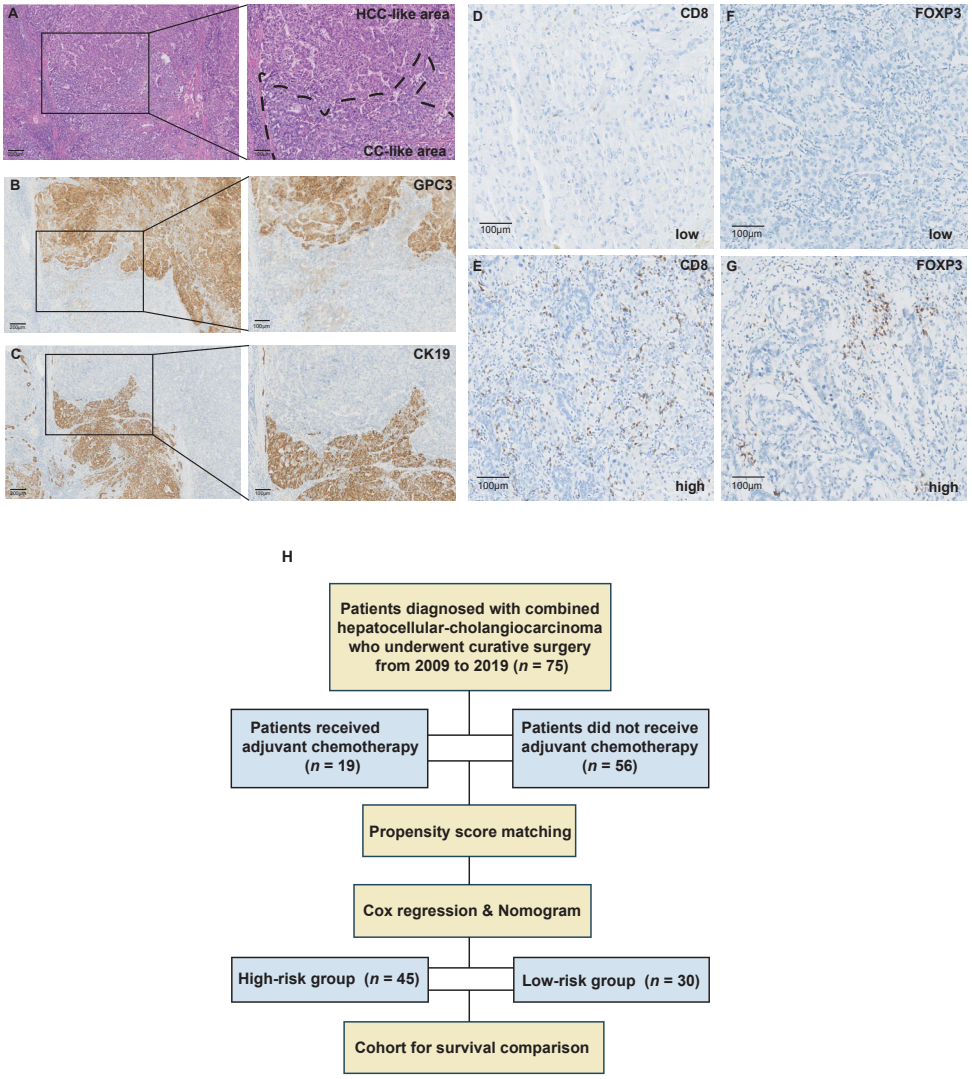

Figure 1. Histopathological features and study design of patients with cHCC-CCA. (A) H&E staining showing distinct HCC-like and CC-like regions. **(B–C)** GPC3 and CK19 immunostaining confirming dual hepatocellular and cholangiocellular phenotypes. **(D–G)** CD8 and FOXP3 staining indicating low and high immune cell infiltration. **(H)** Study flowchart: patient selection, treatment grouping, risk stratification, and PSM.

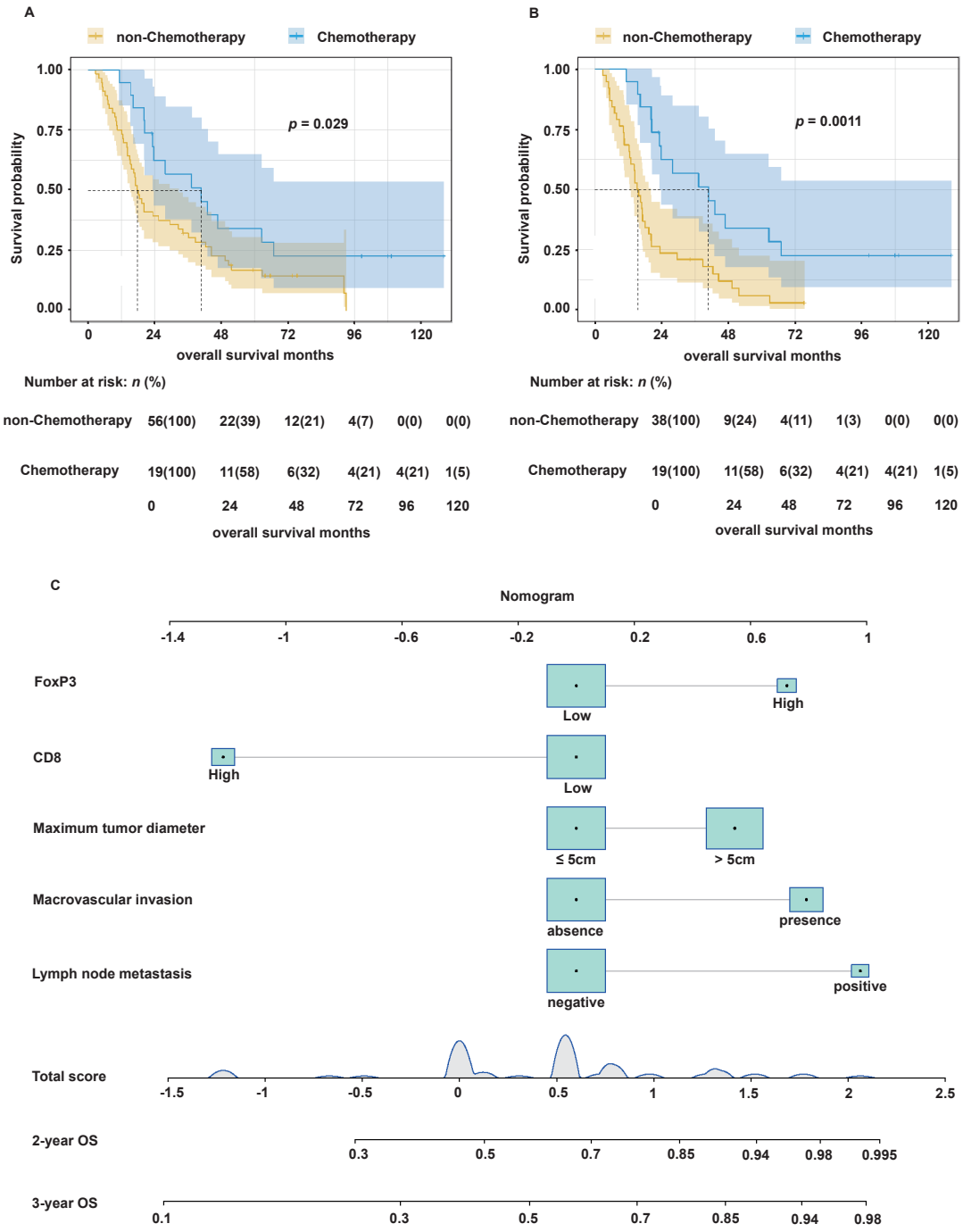

Figure 2. Survival outcomes and prognostic nomogram. (A) Kaplan–Meier curve comparing chemotherapy vs. non-chemotherapy in the unmatched cohort. **(B)** Kaplan–Meier curve after PSM showing improved survival with chemotherapy. **(C)** Nomogram incorporating five variables to predict 2- and 3-year overall survival.

10.5%, $p = 0.869$), or macrovascular invasion (26.3% *vs*. 23.7%, $p = 1.000$).

Regarding immune microenvironment markers, the high expression of CD8 was observed in 5.3% of patients in the chemotherapy group and 0% in the non-chemotherapy group ($p = 0.3330$). The high expression of FOXP3 was observed in 5.3% and 2.6% of patients, respectively ($p = 1.000$). The results of PSM-matched survival analysis indicated that patients who received adjuvant chemotherapy had significantly better overall survival than those who did not ($p = 0.0011$) (Figure 2B), further confirming the survival benefit of adjuvant chemotherapy.

3.3. Construction of the nomogram model

Univariate and multivariate Cox regression analyses were conducted to determine independent prognostic factors for OS. The univariate analysis (Table 2) revealed that macrovascular invasion (HR = 1.767, 95% CI: 1.015–3.076, $p = 0.044$), lymph node metastasis (HR = 2.596, 95% CI: 1.099–6.132, $p = 0.030$), the largest

Table 1. Clinicopathologic characteristics of patients in two groups

Characteristic	Median (IQR) or number (%)		*p*-value
	Chemotherapy group (*n* =19)	Non-Chemotherapy group (*n* =38)	
Sex			0.553
Male	14 (73.7)	32 (84.2)	
Female	5 (26.3)	6 (15.8)	
Age	54 (49-65)	55.5 (52-63)	0.617
HBV			0.887
Present	13 (68.4)	27 (71.1)	
Absent	6 (31.6)	11 (28.9)	
Liver cirrhosis			0.695
Present	6 (31.6)	14 (36.8)	
Absent	13 (68.4)	24 (63.2)	
ALB (g/L)	43.1 (38.1-48.0)	41.85 (39.125-44.275)	0.326
TBIL (μmol/L)	19.0 (13.3-22.9)	16.8 (12.775-21.25)	0.660
PT (sec)	11.1 (10.6-11.8)	11.2 (10.9-11.7)	0.209
AFP (ng/mL)			0.061
> 40	6 (31.6)	22 (57.9)	
≤ 40	13 (68.4)	16 (42.1)	
Satellite lesions			0.906
Present	3 (15.8)	8 (21.1)	
Absent	16 (84.2)	30 (78.9)	
Microvascular invasion			0.869
Present	1 (5.3)	4 (10.5)	
Absent	18 (94.7)	34 (89.5)	
Macrovascular invasion			1.000
Present	5 (26.3)	9 (23.7)	
Absent	14 (73.7)	29 (76.3)	
Lymphatic node metastasis			0.170
Present	4 (21.1)	2 (5.3)	
Absent	15 (78.9)	36 (94.7)	
Largest tumor size (cm)			0.707
>5	11 (57.9)	20 (52.6)	
≤5	8 (42.1)	18 (47.4)	
CD8			0.333
High	1 (5.3)	0	
Low	18 (94.7)	38 (100)	
CD20			0.523
High	6 (31.6)	9 (23.7)	
Low	13 (68.4)	29 (76.3)	
FOXP3			1.000
High	1 (5.3)	1 (2.6)	
Low	18 (94.7)	37 (97.4)	
PD-L1			1.000
High	2 (10.5)	4 (10.5)	
Low	17 (89.5)	34 (89.5)	

Abbreviation: IQR, interquartile ranges; HBV, Hepatitis B Virus; ALB, albumin; TBIL, total bilirubin; PT, prothrombin time; AFP, alpha-fetoprotein.

tumor size > 5 cm (HR = 1.640, 95% CI: 0.993–2.709, p = 0.053), the high expression of CD8 (HR = 0.407, 95% CI: 0.174–0.951, p = 0.038), and the high expression of FOXP3 (HR = 1.935, 95% CI: 0.825–4.537, p = 0.129) were linked to OS..

Multivariate Cox analysis further confirmed that macrovascular invasion (HR = 1.964, 95% CI: 1.074–3.591, p = 0.028), lymph node metastasis (HR = 3.712, 95% CI: 1.424–9.674, p = 0.007), the largest tumor size > 5 cm (HR = 1.661, 95% CI: 1.001–2.768, p = 0.050), the high expression of CD8 (HR = 0.285, 95% CI: 0.113–0.718, p = 0.008), and the high expression of FOXP3 (HR = 3.350, 95% CI: 1.192–9.415, p = 0.022) were independent prognostic factors (Table 2).

Based on these five independent prognostic factors, a nomogram was developed to predict the 2- and 3-year survival rates (Figure 2C). Lymph node metastasis, macrovascular invasion, the largest tumor size diameter > 5 cm, and the high expression of FOXP3 had adverse effects on prognosis, while the high expression of CD8 was a beneficial prognostic factor.

3.4. Validation of the nomogram model

The calibration curves for predicting the 2-year and 3-year OS closely matched the ideal 45-degree reference line, demonstrating excellent agreement between the predicted and observed survival probabilities (Figures

Table 2. Univariate and multivariate analyses of prognostic factors based on OS

Variable	Univariate		Multivariate	
	HR (95%CI)	*p*-value	HR (95%CI)	*p*-value
Sex				
Male	Reference		Reference	
Female	1.594 (0.877-2.896)	0.126	1.513 (0.804-2.846)	0.199
Age	1.014 (0.981-1.048)	0.399		
HBV				
Present	Reference			
Absent	0.830 (0.493-1.399)	0.484		
Liver cirrhosis				
Present	Reference			
Absent	1.006 (0.604-1.677)	0.981		
ALB (g/L)	0.972 (0.914-1.034)	0.372		
TBIL (μmol/L)	1.002 (0.982-1.023)	0.819		
PT (sec)	1.013 (0.770-1.334)	0.925		
AFP (ng/ml)				
≤40	Reference			
> 40	1.101 (0.670-1.808)	0.705		
Satellite lesions				
Present	Reference			
Absent	1.027 (0.546-1.929)	0.935		
Microvascular invasion				
Present	Reference			
Absent	1.768 (0.756-4.133)	0.189		
Macrovascular invasion				
Present	Reference		Reference	
Absent	1.767 (1.015-3.076)	0.044	1.964 (1.074-3.591)	0.028
Lymphatic node metastasis				
Present	Reference		Reference	
Absent	2.596 (1.099-6.132)	0.030	3.712 (1.424-9.674)	0.007
Largest tumor size (cm)				
≤ 5	Reference		Reference	
> 5	1.640 (0.993-2.709)	0.053	1.661 (1.001-2.768)	0.050
CD8				
High	Reference		Reference	
Low	0.407 (0.174-0.951)	0.038	0.285 (0.113-0.718)	0.008
CD20				
High	Reference			
Low	0.729 (0.413-1.287)	0.276		
FOXP3				
High	Reference		Reference	
Low	1.935 (0.825-4.537)	0.129	3.350 (1.192-9.415)	0.022
PD-L1				
High	Reference			
Low	1.557 (0.762-3.181)	0.225		

Abbreviation: HR, hazard ratios; HBV, Hepatitis B Virus; ALB, albumin; TBIL, total bilirubin; PT, prothrombin time; AFP, alpha-fetoprotein.

3A and 3B). The DCA further demonstrated that the nomogram model offered greater net clinical benefit in predicting 2- and 3-year OS compared to the "treat-all" or "treat-none" strategies (Figures 3C and 3D). Time-dependent ROC curve analysis indicated an area under the ROC curve (AUC) of 0.694 for 2-year OS and 0.689 for 3-year OS (Figure 3E), indicating moderate predictive accuracy.

3.5. Risk stratification based on the nomogram

Based on the calculated risk scores, the patients were categorized into high- (n = 45) and low-risk (n = 30) groups. Kaplan–Meier survival curves revealed a significantly poorer prognosis for patients in the high-risk group compared to those in the low-risk group (p = 0.00031; Figure 3F), validating the effectiveness of the nomogram stratification.

In the low-risk group, the group that received adjuvant chemotherapy did not demonstrate a superior survival prognosis (p = 0.084) (Figure 4A); conversely, in the high-risk group, patients who underwent adjuvant chemotherapy exhibited significantly improved survival compared to those who did not undergo adjuvant chemotherapy (p = 0.013) (Figure 4B).

4. Discussion

cHCC-CCA is a rare primary liver malignancy characterized by the coexistence of HCC and CCA

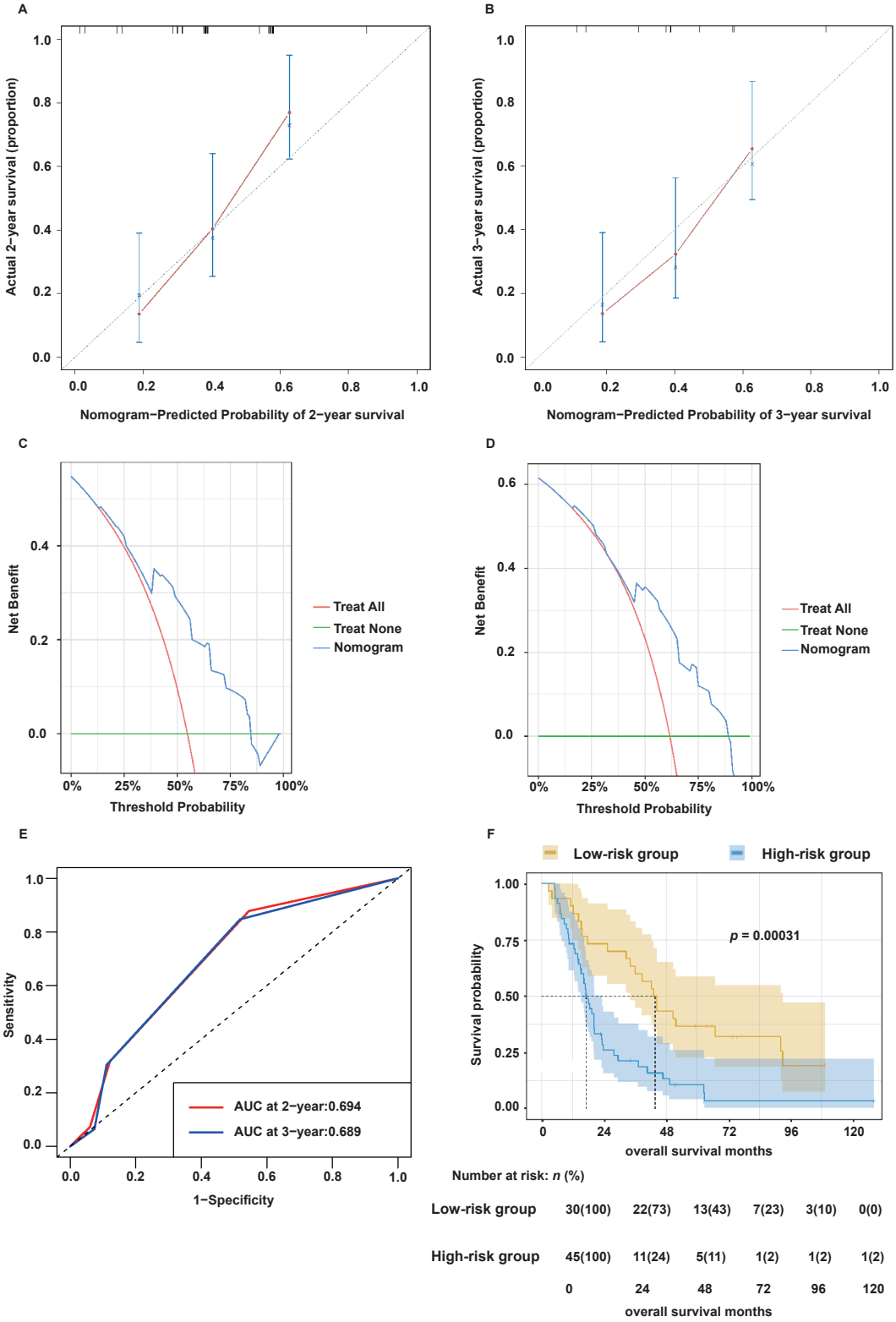

Figure 3. Nomogram validation and risk stratification. (A–B) Calibration plots for 2- and 3-year survival. **(C–D)** Decision curve analysis (DCA) showing clinical utility of the nomogram. **(E)** ROC curves with AUCs of 0.694 (2-year) and 0.689 (3-year). **(F)** Kaplan–Meier curve showing worse survival in the high-risk group.

components. Owing to its complex molecular features and dual histological differentiation, cHCC-CCA displays more aggressive biological behavior, a higher postoperative recurrence rate, and significantly poorer long-term survival compared to either HCC or CCA alone. Curative resection is the sole potentially effective treatment for cHCC-CCA; however, the postoperative recurrence rate exceeds 50%, and there is no established standard adjuvant therapy (*1,21,26*). Enhancing postoperative survival through adjuvant interventions

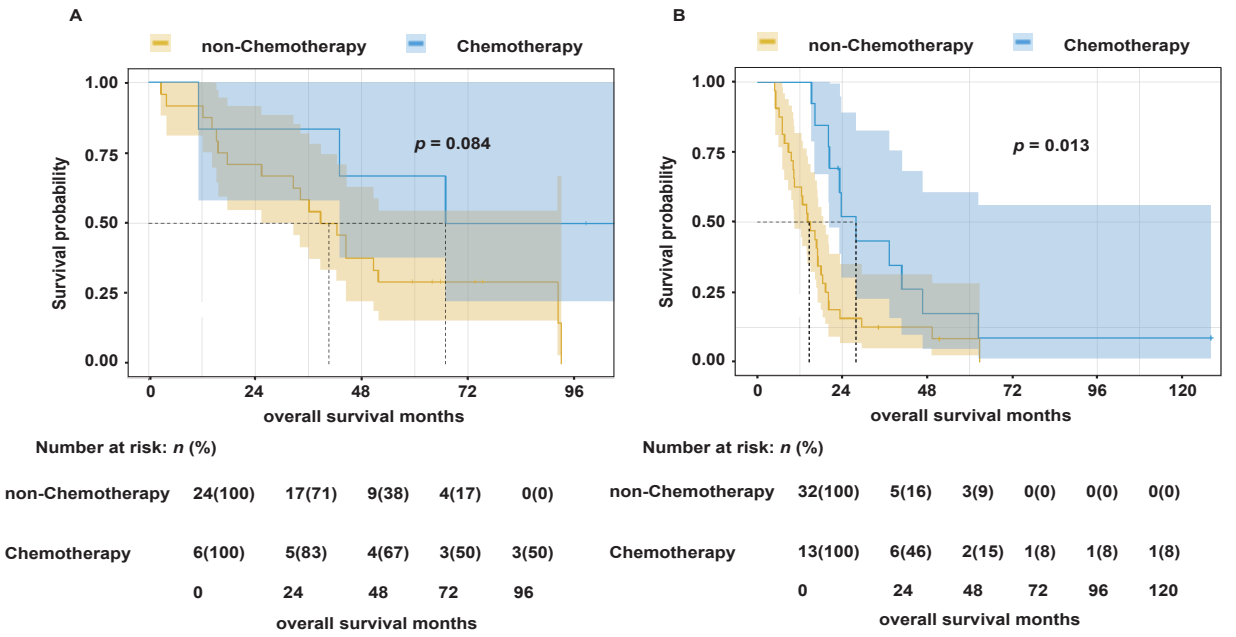

Figure 4. Subgroup survival analysis by risk classification. (A) No significant survival difference in the low-risk group (p = 0.084). **(B)** Chemotherapy significantly improved survival in the high-risk group (p = 0.013).

poses a critical clinical challenge.

In this study, we systematically evaluated the survival benefits of adjuvant chemotherapy after resection in cHCC-CCA patients and established a robust nomogram-based prognostic model using real-world clinical data. This model provides a practical and scientifically grounded tool for individualized postoperative management of patients with cHCC-CCA.

Our main findings showed that adjuvant chemotherapy significantly enhanced the OS of patients with cHCC-CCA. Notably, survival benefits were evident in both high- and low-risk subgroups identified using the nomogram model. This survival benefit remained statistically significant even after PSM, which effectively reduced confounding factors (p = 0.029). In contrast to prior studies with small sample sizes and limited stratified analysis, our study employed robust statistical methods and thorough subgroup analyses, offering more compelling evidence to support the clinical use of adjuvant chemotherapy in cHCC-CCA (*3,27*).

For the development of the prognostic model, we integrated traditional clinicopathological factors like macrovascular invasion, lymph node metastasis, and the largest tumor size, alongside novel immune microenvironment-related markers such as CD8 and FOXP3. Subsequent multivariate Cox regression analysis validated the high expression of CD8 as a favorable prognostic factor (HR = 0.285, p = 0.008), while identifying the high expression of FOXP3 as an independent adverse prognostic factor (HR = 3.350, p = 0.022). These results emphasize the pivotal role of the tumor immune microenvironment in the prognosis of cHCC-CCA and propose potential targets for forthcoming immunotherapy strategies (*23*).

The developed nomogram model exhibited strong predictive performance. Time-dependent ROC curve analyses indicated moderate predictive accuracy, with AUC values of 0.694 for 2-year OS and 0.689 for 3-year OS. Calibration curves demonstrated excellent concordance between predicted survival probabilities and actual outcomes. Decision curve analysis (DCA) illustrated that the nomogram model yielded superior clinical net benefit compared with conventional staging systems for both 2-year and 3-year survival predictions. The population can be stratified into high- and low-risk categories based on the nomogram scores. Postoperative adjuvant chemotherapy did not confer a significant survival benefit for patients in the low-risk category. These results highlight the model's potential as a reliable and intuitive clinical tool to guide personalized treatment decisions and accurately evaluate the benefits of adjuvant chemotherapy.

Despite the significant findings of this study, there are several limitations. Firstly, it was retrospective and carried out at a single center with a relatively small sample size, potentially introducing a selection bias. Secondly, the small sample size utilized for identifying immune microenvironment markers may have impacted the model's generalizability. Lastly, external validation with independent multicenter prospective cohorts is necessary to validate the model's robustness and broader applicability.

In summary, this study not only systematically verified, for the first time, the important role of adjuvant chemotherapy in postoperative survival benefits in cHCC-CCA but also successfully constructed a

prognostic prediction model based on clinicopathological features and immune microenvironmental indices, which possesses good predictive ability and clinical practicability and can screen out the patient population that can benefit from adjuvant chemotherapy(*28*). Future studies should focus on integrating multi-omics data, such as genomic, transcriptomic, and proteomic profiles, and conduct large-scale prospective validations to further optimize and refine the prognostic models. These efforts will ultimately contribute to the advancement of precision medicine and standardized management strategies for patients with postoperative cHCC-CCA, thereby improving long-term survival outcomes (*29*).

Our study showed that adjuvant chemotherapy markedly enhanced postoperative OS in patients with cHCC-CCA. Furthermore, the nomogram model, developed using multivariate analysis, exhibited excellent predictive performance and strong clinical applicability, offering an efficient tool for personalized survival prediction and adjuvant treatment decision-making in cHCC-CCA patients. This model is of significant value for clinical implementation and the progression of precision medicine in cHCC-CCA management.

Acknowledgements

Lu Chen would like to thank the 2023/2024 IHPBA Kenneth Warren Fellowship for the financial support.

Funding: This work was supported by the National Natural Science Foundation of China (grants 82373365, 82173317, 82203423, 82472991 and 82372894), Tianjin Natural Science Foundation (23JCYBJC00600), Joint Funds of the Natural Science Foundation of Tianjin (No.25JCLZJC00350), Tianjin Key Medical Discipline Construction Project (TJYXZDXK-009A).

Conflict of Interest: The authors have no conflicts of interest to disclose.

References

1. Beaufrère A, Calderaro J, Paradis V. Combined hepatocellular-cholangiocarcinoma: An update. J Hepatol. 2021; 74:1212-1224.
2. Calderaro J, Ghaffari Laleh N, Zeng Q, *et al*. Deep learning-based phenotyping reclassifies combined hepatocellular-cholangiocarcinoma. Nat Commun. 2023; 14:8290.
3. Li X, Ramadori P, Pfister D, Seehawer M, Zender L, Heikenwalder M. The immunological and metabolic landscape in primary and metastatic liver cancer. Nat Rev Cancer. 2021; 21:541-557.
4. Xue R, Chen L, Zhang C, *et al*. Genomic and Transcriptomic Profiling of Combined Hepatocellular and Intrahepatic Cholangiocarcinoma Reveals Distinct Molecular Subtypes. Cancer Cell. 2019; 35:932-947.e938.
5. Nguyen CT, Caruso S, Maille P, *et al*. Immune Profiling of Combined Hepatocellular- Cholangiocarcinoma Reveals Distinct Subtypes and Activation of Gene Signatures Predictive of Response to Immunotherapy. Clin Cancer Res. 2022; 28:540-551.
6. Harding JJ, Khalil DN, Fabris L, Abou-Alfa GK. Rational development of combination therapies for biliary tract cancers. J Hepatol. 2023; 78:217-228.
7. Gong W, Zhang S, Tian X, Chen W, He Y, Chen L, Ding T, Ren P, Shi L, Wu Q, Sun Y, Chen L, Guo H. Tertiary lymphoid structures as a potential prognostic biomarker for combined hepatocellular-cholangiocarcinoma. Hepatol Int. 2024; 18:1310-1325.
8. Chen X, Dong L, Chen L, *et al*. Epigenome-wide development and validation of a prognostic methylation score in intrahepatic cholangiocarcinoma based on machine learning strategies. Hepatobiliary Surg Nutr. 2023; 12:478-494.
9. Chen L, Yin G, Wang Z, Liu Z, Sui C, Chen K, Song T, Xu W, Qi L, Li X. A predictive radiotranscriptomics model based on DCE-MRI for tumor immune landscape and immunotherapy in cholangiocarcinoma. Biosci Trends. 2024; 18:263-276.
10. Yang S, Qian L, Li Z, *et al*. Integrated Multi-Omics Landscape of Liver Metastases. Gastroenterology. 2023; 164:407-423.e417.
11. Dar FS, Abbas Z, Ahmed I, *et al*. National guidelines for the diagnosis and treatment of hilar cholangiocarcinoma. World J Gastroenterol. 2024; 30:1018-1042.
12. Ye L, Schneider JS, Ben Khaled N, Schirmacher P, Seifert C, Frey L, He Y, Geier A, De Toni EN, Zhang C, Reiter FP. Combined Hepatocellular-Cholangiocarcinoma: Biology, Diagnosis, and Management. Liver Cancer. 2024; 13:6-28.
13. Jeong H, Kim KP, Jeong JH, Hwang DW, Lee JH, Kim KH, Moon DB, Lee MA, Park SJ, Chon HJ, Park JH, Lee JS, Ryoo BY, Yoo C. Adjuvant gemcitabine plus cisplatin versus capecitabine in node-positive extrahepatic cholangiocarcinoma: the STAMP randomized trial. Hepatology. 2023; 77:1540-1549.
14. Leone V, Ali A, Weber A, Tschaharganeh DF, Heikenwalder M. Liver Inflammation and Hepatobiliary Cancers. Trends Cancer. 2021; 7:606-623.
15. Trikalinos NA, Zhou A, Doyle MBM, Fowler KJ, Morton A, Vachharajani N, Amin M, Keller JW, Chapman WC, Brunt EM, Tan BR. Systemic Therapy for Combined Hepatocellular-Cholangiocarcinoma: A Single-Institution Experience. J Natl Compr Canc Netw. 2018; 16:1193-1199.
16. Kataoka K, Mori K, Nakamura Y, *et al*. Survival benefit of adjuvant chemotherapy based on molecular residual disease detection in resected colorectal liver metastases: subgroup analysis from CIRCULATE-Japan GALAXY. Ann Oncol. 2024; 35:1015-1025.
17. Moris D, Palta M, Kim C, Allen PJ, Morse MA, Lidsky ME. Advances in the treatment of intrahepatic cholangiocarcinoma: An overview of the current and future therapeutic landscape for clinicians. CA Cancer J Clin. 2023; 73:198-222.
18. Stoop TF, Sugawara T, Oba A, *et al*. Adjuvant Chemotherapy After Resection of Localized Pancreatic Adenocarcinoma Following Preoperative FOLFIRINOX. JAMA Oncol. 2025; 11:276-287.
19. He GQ, Li Q, Jing XY, Li J, Gao J, Guo X. Persistent response to combination therapy of pemigatinib and chemotherapy in a child of combined hepatocellular-cholangiocarcinoma with FGFR2 fusion. Mol Cancer. 2024; 23:269.

20. Rosenberg N, Van Haele M, Lanton T, *et al*. Combined hepatocellular-cholangiocarcinoma derives from liver progenitor cells and depends on senescence and IL-6 trans-signaling. J Hepatol. 2022; 77:1631-1641.
21. Pinter M, Scheiner B, Pinato DJ. Immune checkpoint inhibitors in hepatocellular carcinoma: emerging challenges in clinical practice. Lancet Gastroenterol Hepatol. 2023; 8:760-770.
22. Gan X, Dong W, You W, Ding D, Yang Y, Sun D, Li W, Ding W, Liang Y, Yang F, Zhou W, Dong H, Yuan S. Spatial multimodal analysis revealed tertiary lymphoid structures as a risk stratification indicator in combined hepatocellular-cholangiocarcinoma. Cancer Lett. 2024; 581:216513.
23. Calderaro J, Di Tommaso L, Maillé P, *et al*. Nestin as a diagnostic and prognostic marker for combined hepatocellular-cholangiocarcinoma. J Hepatol. 2022; 77:1586-1597.
24. Heng Q, Hou M, Leng Y, Yu H. Establishment of a prognostic nomogram and risk stratification system for patients with combined hepatocellular-cholangiocarcinoma. Sci Rep. 2025; 15:16726.
25. Heinze G, Wallisch C, Dunkler D. Variable selection – A review and recommendations for the practicing statistician. Biom J. 2018; 60:431-449.
26. Claasen M, Ivanics T, Beumer BR, de Wilde RF, Polak WG, Sapisochin G, JNM IJ. An international multicentre evaluation of treatment strategies for combined hepatocellular-cholangiocarcinoma(☆). JHEP Rep. 2023; 5:100745.
27. Kelley RK, Rimassa L, Cheng AL, *et al*. Cabozantinib plus atezolizumab versus sorafenib for advanced hepatocellular carcinoma (COSMIC-312): a multicentre, open-label, randomised, phase 3 trial. Lancet Oncol. 2022; 23:995-1008.
28. Yang H, Cheng J, Zhuang H, *et al*. Pharmacogenomic profiling of intra-tumor heterogeneity using a large organoid biobank of liver cancer. Cancer Cell. 2024; 42:535-551.e538.
29. Liu Q, Zhang X, Qi J, *et al*. Comprehensive profiling of lipid metabolic reprogramming expands precision medicine for HCC. Hepatology. 2025; 81:1164-1180.

Received June 23, 2025; Revised July 10, 2025; Accepted July 14, 2025.

[§]These authors contributed equally to this work.

**Address correspondence to:*
Xiangdong Tian, Wenchen Gong, and Lu Chen, Tianjin Medical University Cancer Institute and Hospital, West Huan-Hu Road, Ti Yuan Bei, Hexi District, Tianjin 300060, China.
E-mail: xiangdongtian@tmu.edu.cn (XT); gongwenchen@tmu.edu.cn (WG); chenlu@tmu.edu.cn (LC)

Released online in J-STAGE as advance publication July 16, 2025.